

Controlled assembly of In₂O₃ nanowires on electronic circuits using scanning optical tweezers

Song-Woo Lee¹, Gunho Jo², Takhee Lee,²
and Yong-Gu Lee^{1,*}

¹Department of Mechatronics, Gwangju Institute of Science and Technology (GIST),
1 Oryong-dong, Buk-gu, Gwangju, 500-712, Korea

²Department of Material Science and Engineering, Gwangju Institute of Science and Technology (GIST),
1 Oryong-dong, Buk-gu, Gwangju, 500-712, Korea

*lygu@gist.ac.kr

Abstract: In₂O₃ nanowires can be used effectively as building blocks in the production of electronic circuits used in transparent and flexible electronic devices. The fabrication of these devices requires a controlled assembly of nanowires at crucial places and times. However, this kind of controlled assembly, which results in the fusion of nanowires to circuits, is still very difficult to execute. In this study, we demonstrate the benefits of using various lengths of In₂O₃ nanowires by using non-contact mechanisms, such as scanning optical tweezers, to place them on designated targets during the fabrication process. Furthermore, these nanowires can be stabilized at both ends of the conducting wires using a focused laser, and later in the process, the annealed technique, so that proper flow of electrons is affected.

©2009 Optical Society of America

OCIS codes: (350.4855) Optical tweezers or optical manipulation; (120.4610) Optical fabrication.

References and links

1. G. Jo, W.-K. Hong, J. Maeng, T.-W. Kim, G. Wang, A. Yoon, S.-S. Kwon, S. Song, and T. Lee, "Structural and electrical characterization of intrinsic n-type In₂O₃ nanowires," *Colloids and Surfaces A* **313–314**, 308–311 (2008).
2. G. Jo, W.-K. Hong, J. I. Sohn, M. Jo, J. Shin, M. E. Welland, H. Hwang, K. E. Geckeler, and T. Lee, "Hybrid complementary logic circuits of one-dimensional nanomaterials with adjustment of operation voltage," *Adv. Mater.* **21**(21), 2156–2160 (2009).
3. S. Ju, A. Facchetti, Y. Xuan, J. Liu, F. Ishikawa, P. Ye, C. Zhou, T. J. Marks, and D. B. Janes, "Fabrication of fully transparent nanowire transistors for transparent and flexible electronics," *Nat. Nanotechnol.* **2**(6), 378–384 (2007).
4. Y. Huang, X. Duan, Y. Cui, L. J. Lauhon, K.-H. Kim, and C. M. Lieber, "Logic gates and computation from assembled nanowire building blocks," *Science* **294**(5545), 1313–1317 (2001).
5. G. Jo, J. Maeng, T.-W. Kim, W.-K. Hong, M. Jo, H. Hwang, and T. Lee, "Effects of channel-length scaling on In₂O₃ nanowire field effects transistors studied by conducting atomic force microscopy," *Appl. Phys. Lett.* **90**(17), 173106 (2007).
6. W. U. Wang, C. Chen, L. Keng-hui, Y. Fang, and C. M. Lieber, "Label-free detection of small-molecule-protein interactions by using nanowire nanosensors," in *Proceeding of the National Academy of Sciences of the USA* **102**, 3208–3212 (2005).
7. E. C. Walter, F. Favier, and R. M. Penner, "Palladium mesowire arrays for fast hydrogen sensors and hydrogen-actuated switches," *Anal. Chem.* **74**(7), 1546–1553 (2002).
8. A. M. Zaitsev, A. M. Levine, and S. H. Zaidi, "Temperature and chemical sensor based on FIB-written carbon nanowires," *IEEE Sensors* **8**(6), 849–856 (2008).
9. N. Kouklin, L. Menon, A. Z. Wong, D. W. Thompson, J. A. Woollam, P. F. Williams, and S. Bandyopadhyay, "Giant photoresistivity and optically controlled switching in self-assembled nanowires," *Appl. Phys. Lett.* **79**(26), 4423–4425 (2001).
10. Q. Li, and V. W.-W. Yam, "Redox luminescence switch based on energy transfer in CePO₄:Tb³⁺ nanowires," *Angew. Chem.* **119**(19), 3556–3559 (2007).
11. H. Bao, C. M. Li, X. Cui, Q. Song, H. Yang, and J. Guo, "Single-crystalline Bi₂S₃ nanowire network film and its optical switches," *Nanotechnology* **19**(33), 335302 (2008).
12. D. Whang, S. Jin, Y. Wu, and C. M. Lieber, "Large-scale hierarchical organization of nanowire arrays for integrated nanosystems," *Nano Lett.* **3**(9), 1255–1259 (2003).

13. A. Tao, F. Kim, C. Hess, J. Goldberger, R. He, Y. Sun, Y. Xia, and P. Yang, "Langmuir-Blodgett silver nanowire monolayers for molecular sensing using surface-enhanced Raman spectroscopy," *Nano Lett.* **3**(9), 1229–1233 (2003).
14. Y. Huang, X. Duan, Q. Wei, and C. M. Lieber, "Directed assembly of one-dimensional nanostructures into functional networks," *Science* **291**(5504), 630–633 (2001).
15. P. A. Smith, C. D. Nordquist, T. N. Jackson, T. S. Mayer, B. R. Martin, J. Mbindyo, and T. E. Mallouk, "Electric-field assisted assembly and alignment of metallic nanowires," *Appl. Phys. Lett.* **77**(9), 1399–1401 (2000).
16. X. Duan, Y. Huang, Y. Cui, J. Wang, and C. M. Lieber, "Indium phosphide nanowires as building blocks for nanoscale electronic and optoelectronic devices," *Nature* **409**(6816), 66–69 (2001).
17. A. Jamshidi, P. J. Pauzauskie, P. J. Schuck, A. T. Ohta, P.-Y. Chiou, J. Chou, P. Yang, and M. C. Wu, "Dynamic manipulation and separation of individual semiconducting and metallic nanowires," *Nat. Photonics* **2**(2), 86–89 (2008).
18. A. T. Ohta, S. L. Neale, H.-Y. Hsu, J. K. Valley, and M. C. Wu, "Parallel assembly of nanowires using lateral-field optoelectronic tweezers," in *Proceedings of the IEEE/LEOS Optical MEMS and Nanophotonics* (Freiburg, Germany 2008), pp. 7–8.
19. R. C. Gauthier, M. Ashman, and C. P. Grover, "Experimental confirmation of the optical-trapping properties of cylindrical objects," *Appl. Opt.* **38**(22), 4861–4869 (1999).
20. R. C. Gauthier, "Optical levitation and trapping of a micro-optic inclined end-surface cylindrical spinner," *Appl. Opt.* **40**(12), 1961–1973 (2001).
21. R. Agarwal, K. Ladavac, Y. Roichman, G. Yu, C. M. Lieber, and D. G. Grier, "Manipulation and assembly of nanowires with holographic optical traps," *Opt. Express* **13**(22), 8906–8912 (2005).
22. T. Yu, F.-C. Cheong, and C.-H. Sow, "The manipulation and assembly of CuO nanorods with line optical tweezers," *Nanotechnology* **15**(12), 1732–1736 (2004).
23. ChanHyuk Nam, Dongjin Lee, Daehie Hong and Jong-Heun Lee, "Manipulation of nano devices with optical tweezers," in *Proceeding of Nanoengineering Symposium* (Daejeon, Korea, 2005), pp. 387–391.
24. P. J. Pauzauskie, A. Radenovic, E. Trepagnier, H. Shroff, P. Yang, and J. Liphardt, "Optical trapping and integration of semiconductor nanowire assemblies in water," *Nat. Mater.* **5**(2), 97–101 (2006).
25. A. Balijepalli, T. W. LeBrun, and S. K. Gupta, "A flexible system framework for a nanoassembly cell using optical tweezers," in *Proceedings of the ASME Design Engineering Technical Conference* (Philadelphia, Pennsylvania, USA 2006).
26. A. van der Horst, A. I. Campbell, L. K. van Vugt, D. A. M. Vanmaekelbergh, M. Dogterom, and A. van Blaaderen, "Manipulating metal-oxide nanowires using counter-propagating optical line tweezers," *Opt. Express* **15**(18), 11629–11639 (2007).
27. J. Plewa, E. Tanner, D. M. Mueth, and D. Grier, "Processing carbon nanotubes with holographic optical tweezers," *Opt. Express* **12**(9), 1978–1981 (2004).
28. S.-W. Lee, T. Lee, and Y.-G. Lee, "Stable manipulating of nanowires by line optical tweezers with haptic feedback," *Proc. SPIE* **6644**, 66441X (2007).
29. F. Borghese, P. Denti, R. Saija, M. A. Iati, and O. M. Maragò, "Radiation torque and force on optically trapped linear nanostructures," *Phys. Rev. Lett.* **100**(16), 163903 (2008).
30. A. Rohrbach, "Stiffness of optical traps: quantitative agreement between experiment and electromagnetic theory," *Phys. Rev. Lett.* **95**(16), 168102 (2005).
31. F. Borghese, P. Denti, R. Saija, and M. A. Iati, "Optical trapping of nonspherical particles in the T-matrix formalism: erratum," *Opt. Express* **15**(22), 14618 (2007).
32. F. Borghese, P. Denti, R. Saija, and M. A. Iati, "Radiation torque on nonspherical particles in the transition matrix formalism," *Opt. Express* **14**(20), 9508–9521 (2006).

1. Introduction

Nanowires are one-dimensional structures with diameters in nanometer scale and have a diameter to length ratio of over one-hundred to one. Furthermore, because of their unique morphology, they exhibit extraordinary electrical and mechanical properties. Nanowires can be used to build nanoscale devices such as electric devices [1–5], nanosensors [6–8], and nano switches [9–11] but may have unforeseen consequences which require specific intervention. Consequently, techniques incorporating controlled manipulation of nanowires are crucial to ensure that these intervention techniques are effective. Unfortunately, contact type manipulation is difficult at this scale because of the stiction forces between the grippers and the nanowires. Due to this obstacle, non-contact techniques such as the Langmuir-Blodgett method [12,13], the fluidic flow method [14], manipulations based on electric-fields [15–18], and the use of optical tweezers [19–28] are receiving more attention.

The Langmuir-Blodgett method disperses nanowires on a solution surface around which two parallel barriers are then closed to effectively direct the nanowires between the barriers [12]. In the fluidic flow method, the fluidic medium flows in a constant direction, and nanowires are then aligned to flow with the streamline. Huang et al. [14] have used this

method to align a set of nanowires towards one direction, resulting in their chemical immobilization. The Langmuir-Blodgett and fluidic flow methods can be applied to nanowires in bulk but lack individual control which in the end sacrifices quality. Another technique is the use of electric fields which can be applied to align nanowires within the electric fields themselves. In fact, Smith et al. [15] have used electric fields to align Au nanowires between electrode fingers. With the inclusion of opto-electronic tweezers [17], electrode fingers can be moved within the photoconductive layers, aligning the nanowires with them in the process. Nanowires are usually oriented perpendicularly to the photoconductive layers, making it difficult to settle them on electronic circuit patterns, which are usually parallel to these layers, in a controlled manner. However, recent work by Ohta et al. [18] has demonstrated a lateral version of the opto-electronic tweezers that is capable manipulating and orientating nanowires laterally.

The last method employed in non-contact manipulation is the use of optical tweezers which utilize laser beams, strongly focused, to trap and manipulate objects. For the most part, optical tweezers have been used in the past to trap and manipulate spherical micrometer scaled objects such as polystyrene beads. Lately, however, they have been extended to include non-spherical objects such as nanowires. The use of this technique allows nanowires to be manipulated so that any desired direction and orientation becomes possible, the advantage being more individual control. Agarwal et al. [21] have used holographic optical tweezers to devise multiple traps which are then spanned on CdS nanowires to trap and manipulate objects. They have been able to demonstrate the simultaneous trapping and manipulation of two nanowires in their experimentation. Furthermore, nanowires have been cut and fused at junctions using high-powered lasers. On the other hand, Yu et al. [22] have used line optical tweezers to manipulate CuO nanorods. In their study, nanowires are arranged in common configurations, such as crosses, and they have been able to stabilize nanowires between two electrodes. However, no signs of electrical contact have been detected. In another attempt, Balijepalli et al. [25] have used scanning optical tweezers to trap and rotate Al_2SiO_5 nanowires. Plewa et al. [27] have demonstrated how to shape bundles of carbon nanotubes into various polygonal shapes using holographic optical tweezers. It is important to note that optical tweezers aren't capable of trapping nanowires that possess different geometries and materials [24]. For some nanowires, the scattering forces are far stronger than the gradient forces, effectively making them impossible to trap. However, trapping can occur with some nanowires by utilizing limiting walls, effectively cancelling the forces caused by light scattering. Additionally, some methods require the use of various types of limiting walls during the process of trapping nanowires. Nam et al. [23] have used scanning optical tweezers with the help of limiting coverglass to manipulate SnO_2 nanowires. Pauzauskie et al. [24]. have placed the nanowires horizontally on the coverglass by pushing the top end onto a lysine-coated coverglass, using the end as a pivot to rotate both ends until contact is made with the coverglass. They have also demonstrated the stable formation of junctions by irradiating them with a high power infrared laser. In another study, van der Horst et al. [26] have used counter-propagating optical line tweezers to manipulate ZnO and silica-coated Si nanowires. Counter-propagating beams act as a virtual limiting wall and cancel out strong scattering forces. Moreover, Lee et al. [28] have demonstrated the manipulation of In_2O_3 nanowires by using scanning optical tweezers with haptic feedback. In their work, sense of torque and force have been experienced by the user where the torque and force magnitude is proportional to the gap between the command and the actual movement of the nanowire.

In order to construct nanoscale devices, the features which are necessary for effective manipulation of nanowires are stable grips, accurate movement/rotation and the ability to trap nanowires of various diameters and lengths. In this study, we demonstrate the importance of scanning optical tweezers to actively manipulate In_2O_3 nanowires of various dimensions. These In_2O_3 nanowires have proven to be an attractive material in the fabrication of nanoscale devices. Furthermore, these semiconductor nanowires are highly transparent and mechanically flexible. Their transparent characteristic is especially useful in the production of fully transparent nanowire transistors [3].

2. Experimental setup

2.1 Scanning optical tweezers setup

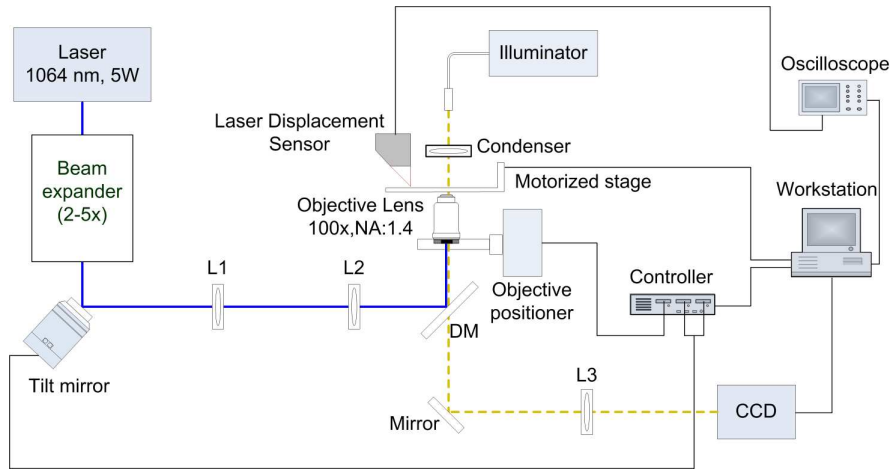


Fig. 1. Experimental setup of the scanning optical tweezers

Figure 1 shows the experimental setup of the scanning optical tweezers. The laser used for this work is a 1064nm fiber laser (B&W TEK Inc, BWC-FL-1064-5 Series). Not shown here, a diode laser beam (Power Tech, 685nm, 50mW) shares the optical path of the trapping laser and a quadrant photodiode (QPD, Thorlabs, PDQ80S1) is placed on the back focal plane to detect nanowire positioning. A band-pass filter blocks the trapping beam from entering into the QPD. A piezoelectric tilt mirror is used to monitor the location of the in-plane (lateral) focal point. A piezoelectric objective positioner is used for the out-of-plane (axial) motions. For high speed control of the two piezoelectric devices, a C-300 series DSP controller is used. The incoming beam is focused and directed towards the sample plane with the help of a high NA (1.4), 100X magnification objective lens. A beam expander (Thorlabs, BE02-05-B) with a magnification of 2~5 is used to overfill the back aperture of the objective lens. For observations of larger sample areas, a three axis motorized stage is used. A high precision optical position sensor (EM4SYS, HIPOPS) is used to monitor the movement of the motorized stage in the vertical axis. The sample, as well as the reflection of the laser from the coverglass, is monitored by a CCD (QImaging, Retiga Exi 1394).

2.2 In_2O_3 nanowires and electronic circuits

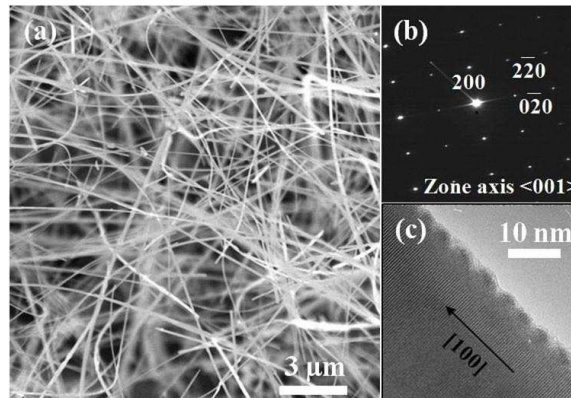


Fig. 2. (a) SEM image of In_2O_3 nanowires. (b) SAED pattern of the In_2O_3 nanowire recorded along the $\langle 001 \rangle$ zone axis. (c) HRTEM image of an In_2O_3 nanowire

The semiconducting In_2O_3 nanowires used in this study are synthesized utilizing a vapor-liquid-solid (VLS) and chemical vapor deposition (CVD) on Au catalysts. Figure 2 shows a typical scanning electron microscopy (SEM) image of In_2O_3 nanowires grown on SiO_2/Si substrate. These nanowires have diameters in the range of 20~200nm and lengths ranging up to tens of micrometers, indicating an aspect ratio of more than 50:1. The highly crystalline nature of these In_2O_3 nanowires are further evident by the selected area electron diffraction (SAED) patterns and the high-resolution transmission of electron microscopy (HR-TEM) images, as shown in Fig. 2 (b) and Fig. 2 (c). Note that the SAED pattern and the HR-TEM image indicate that the In_2O_3 nanowire is made of a single-crystalline material with a growth direction of [100]. A detailed description of the synthesis and characterization of In_2O_3 nanowires has been reported elsewhere [1]. To isolate the nanowires from SiO_2/Si substrate and to disperse them in a solution, the substrate is placed in a bottle containing distilled water and sonified for approximately 1 minute.

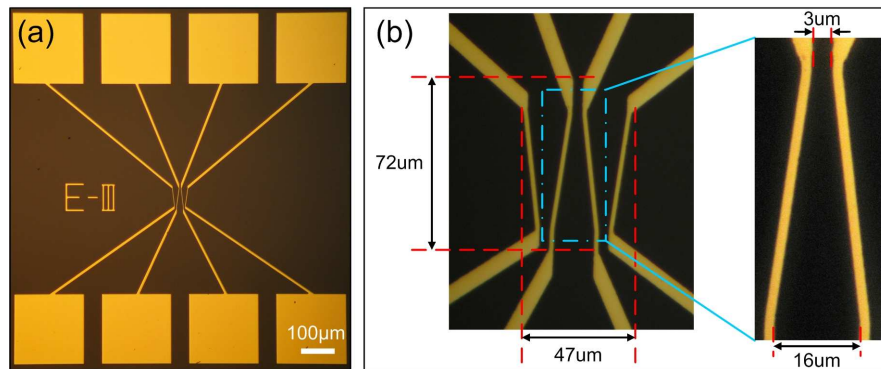


Fig. 3. Electronic circuit composed of varying separations to accommodate various lengths of nanowires

The gold circuit is patterned on a 250nm Au which is deposited on the coverglass. The deposition is achieved by the sputtering process, and Fig. 3 (a) shows the resulting Au electric circuit. The image shown is taken at a 20X magnification. As is clear from the image above, the circuit consists of 4 conducting wires. Both ends of each conducting wire are linked to the electrodes. Figure 3 (b) shows the central portion of the circuit. The central area where experiments are conducted is an area of $72\mu\text{m} \times 47\mu\text{m}$. The design width of each conducting wire, at the center of the circuit, is $1\mu\text{m}$. Since the individual lengths of nanowires vary, conducting wires are arranged in a W-shaped manner at the center of the circuit. As depicted in the figure, the distance between two adjacent conducting wires varies from $3\mu\text{m}$ to $16\mu\text{m}$. The length of the target nanowires attached to this circuit should range at a slightly longer distance than the distance between the two adjacent wires.

The sample chamber is created by a sealed wall of alcohol solvent ink (Monami OHP pen permanent) that surrounds a $5 \times 5\text{mm}$ square hole between two commercial coverglasses, 6cm wide. The lower coverglass is coated with dissolved BSA (Bovine Serum Albumin, Sigma) in deionized water to reduce the stiction of nanowires against the lower coverglass. The ink wall produces a chamber with a height of $50\mu\text{m}$, half the size of double-sided sticky tape walls used by most researchers. However, the upper coverglass on which electrodes are patterned are untreated and, consequently, some nanowires stick to the upper coverglass during the experiments.

3. Experimental methods and results

There is an abundance of computation on radiation force regarding spherical objects, and their positive experimental results are widely accepted [29–32]. However, relatively few computations are performed on nanowires. Recently, Borghese et al. [29] have approximated linear nanostructures and computed the force and torque due to light scattering by using a

chain of small identical spheres. They have shown that linear nanostructures of various refractive indices align to the laser beam axis. In this study, a similar approach is used for the initial trapping of nanowires. The In_2O_3 nanowires used in this study have a refractive index of 2.0 and a length scale of 5~13 μm . For these experiments on trapping, the nanowires are used in an aqueous solution. The nanowires are aligned and stably trapped during the propagation of a singly focused laser beam. By moving the focal point of the beam, 3D manipulation of nanowires can then be realized.

Figure 4 (a) and (b) shows the trapping of an In_2O_3 nanowire using a single laser beam. Figure 4 (a) shows a target nanowire in an aqueous solution suspended parallel to the base plane. Figure 4 (b) shows the trapping of the target nanowire when a single, focused laser is turned on. The nanowire gets aligned to the beam axis then it manipulates the nanowire in lateral directions. Under a single laser beam, nanowires can be translated but cannot be rotated so as to orient themselves parallel to the coverglass. The experimental situation in Fig. 4 (g) shows the upper coverglass with imprinted circuits and the nanowires in the aqueous solution being suspended between the upper and lower coverglasses. The objective for this study is to move and rotate these nanowires so that they are immobilized between two conducting wires. As is clear from the description, this is not possible without the critical rotation of the nanowires. Our solution for this dilemma is to move the nanowires towards the assembly site by using a single focused laser. As explained, this process is employed when the nanowires align axially. In order to glue the nanowires to the conducting wires, we rapidly scan the focus to form a line trap and then attach the trapped nanowire to the upper coverglass, the location of the imprint of the targeted conducting wires. The line trap formation only traps the nanowires when the scattering push is limited by a wall, which in this case is served by the upper coverglass.

Figure 4 (c) and (d) shows the actual rotation of a nanowire. Notice that one end of the line trap, delineated by the counterclockwise arrow, acts as a pivot point while the other end rotates. Figure 4 (e) and (f) shows the translation of nanowires as they are continually pushed against the upper coverglass during rotation and translation. The end points of the line trap are shown as green and red dots in the figure. Readers can notice that the length of the line trap is adjusted to the length of the target nanowire. The scan rate is chosen regardless of the length of the nanowire which ranges from 14Hz up to 34Hz.

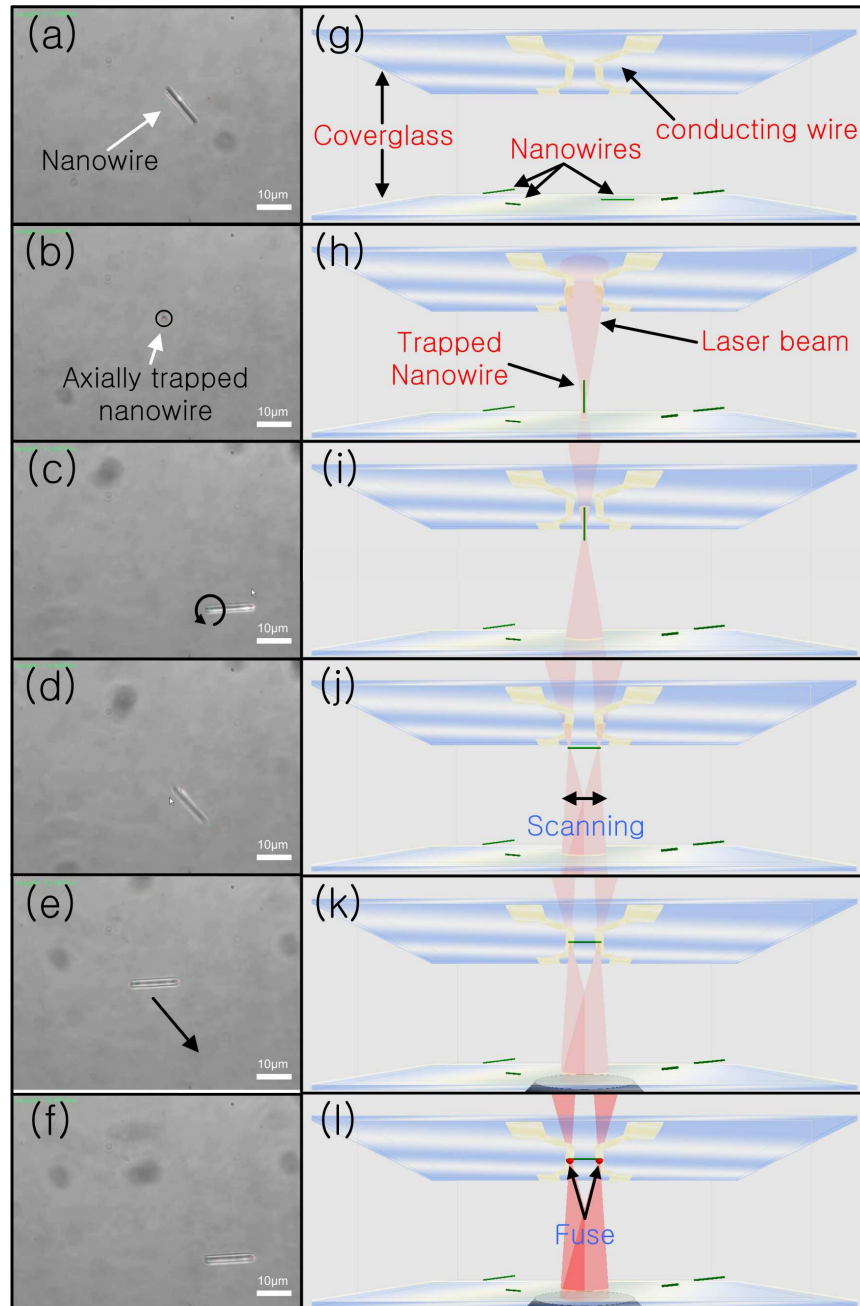


Fig. 4. Manipulation of an axially aligned nanowire. (a) Target Nanowire (b) Axially trapped nanowire (c), (d) Rotation of the nanowire using line optical trap while pushed against the upper coverglass (e), (f) Manipulation of nanowire using line optical trap while pushed against the upper coverglass (g)-(l) Sequence of nanowire assembly

The final goal is to stabilize the fusion of nanowires between two conducting wires, as explained earlier. Figure 4 (g)-(l) shows the schematics of the crucial steps involved in the operation. Figure 4 (g) displays the initial location of the aqueous solution, containing the In_2O_3 nanowires, between the two coverglasses. The electronic circuit is imprinted on the bottom surface of the top coverglass. For this experiment, we find that nanowires are

randomly suspended within the medium, contrary to our previous report [28] where they are resting on the bottom coverglass due to gravitational force. Inconsistency in the location of nanowires within the chamber is caused by differences in the construction methods of the chambers. Previous work used double sided sticky tapes for sealing the chamber whereas current work uses an alcohol solvent ink. Previous chambers are very stable with little evaporation while the current chambers display greater levels of evaporation. Evaporation results in the flow of fluids within the medium and prevented the nanowires to sink down to the bottom of the chamber.

Figure 4 (h) shows the schematic of a single laser focus applied close to the nanowires. This results in the axial alignment of the nanowire placing its lower end on the focal point. The trapped nanowire is then moved to the target site, as shown in Fig. 4 (i), by readjusting the laser focus. We then place the nanowire by rapidly scanning the laser, forming a line trap, as shown in Fig. 4 (j). At this stage, the nanowire is forced towards the upper coverglass as shown in Fig. 4 (k). The trapping power for these steps is kept constant at 1mW. Then, by raising the trapping power to 3.5mW, we are able to fuse the nanowire to the conducting wires as shown in Fig. 4 (l).

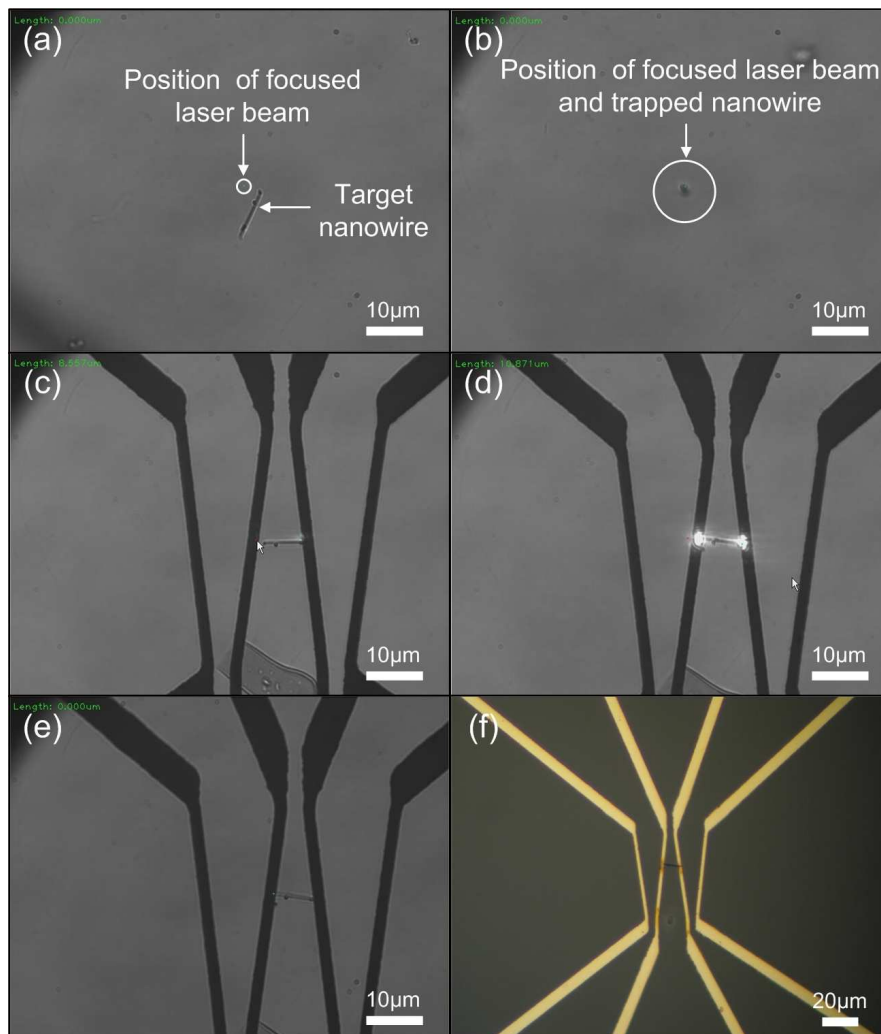


Fig. 5. Trapped and manipulated In_2O_3 nanowire and the formed junction

Figure 5 shows the real experimental images of the schematics, previously shown in Fig. 4 (g)-(l). Figure 5 (a) shows a nanowire resting near the lower coverglass with a focused laser beam nearby. When we approach the nanowire with the focused laser, it is axially aligned as shown in Fig. 5 (b). The nanowire is then moved to the target site and fuses to the conducting wires as shown in Fig. 5 (c), (d). Figure 5 (e) shows the completed fusion of the nanowire on the imprinted Au electric circuit. Figure 5 (f) is a microscopic image of the assembled nanowire which is taken at 50X magnification.

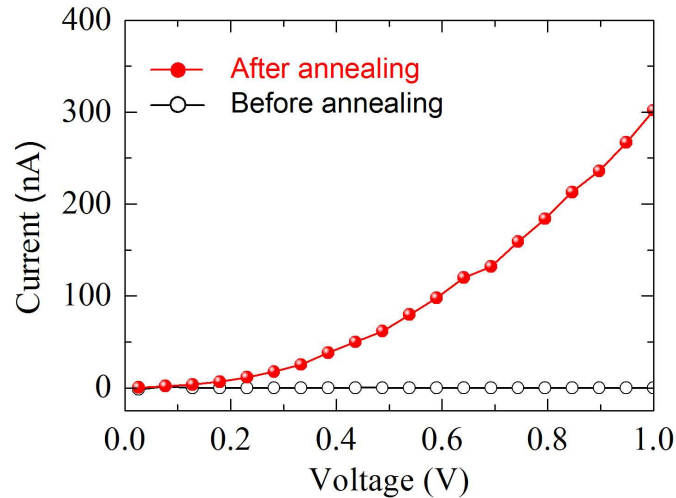


Fig. 6. Current versus voltage (I-V) curves of the In_2O_3 nanowire device

Figure 6 demonstrates the current, versus the voltage (I-V), characteristics of the assembled In_2O_3 nanowire device. Although the nanowire is successfully connected to the two conducting wires (i.e., metal electrodes) using scanning optical tweezers, the current does not flow due to poor electrical contact between nanowire and electrode. Therefore, the In_2O_3 nanowire device is loaded into a graphite schale (thermal annealing device) and is heated to 380°C under the flow of 20scm N_2 for 1 minute to reduce the contact resistance. A lead time of 5 seconds is needed to reach a temperature of 380°C starting at room temperature. After annealing, the conductance of the assembled nanowire device is dramatically increased (the measured current at 0.5V was about 67nA).

We use Au as the contact metal and this creates the Schottky contact, but crosschecking to compare the differences between the contacts is not possible due to a lack of literature. However, a reasonable comparison can be made with the Ohmic contact. The Schottky contact will result in a lower current level than the Ohmic contact. According to Jo et al. [1], an Ohmic contact made by a Ti metal contact showed 500nA at 0.5V. Thus 67nA at 0.5V, demonstrated in our experiment, can be regarded as a reasonable result. In other words, the current level shown in our device should be lower than a Ti or Cr metal contact and this can be verified. In the future, contact metal can be replaced by other materials resulting in better flow of currents. Our focus is to demonstrate a working device fabricated by the controlled assembly of nanowires on circuits using optical tweezers, thus the maximization of the current level is not the prime consideration.

A higher laser power should also result in a more stable trapping of nanowires. This turns out to be true as we conduct the positional error of nanowires from the center as the result of different power from the laser. The positional errors are measured by the QPD (Quadrant Photo Diode) signal in three orthogonal directions and are shown in Fig. 7. Figure 7 is obtained from a single nanowire. Lengths of nanowires vary greatly, thus averaging results from different lengths of nanowire is not helpful to obtain meaningful data. QPD consists of

four quadrants of diodes that independently measure the scattering of nanowires from a detection laser. An X positional error is obtained by subtracting the sum of two quadrants on the left side from the sum of two quadrants on the right side. Y positional error is similarly obtained by subtracting the sum of two quadrants below from the sum of two quadrants above. Z positional error is simply obtained by summing all quadrants together. It is relatively straight forward to obtain a positional error of spherical particles but not as obvious for elongated shapes. The positional errors shown in Fig. 7 pertain to a situation where a nanowire is forced and laid on the surface of the upper coverglass, ending up with its long axis parallel to the X axis. It is, however, not placed symmetrically so that its center is situated on the focal spot of the detection laser. Rather, it is translated so that its left end coincides with the focal spot. We first tried to obtain the X positional error while the nanowire's center is at the focal spot but the difference in signal change was miniscule.

We have not calibrated our system so that the vertical axis in Fig. 7 can be shown in meters. Calibration normally involves using a dried sample placed on a coverglass and assumes the dried sample is identical to the test specimen in terms of shapes and material. However, nanowires are non-uniform in terms of lengths, thus calibration is not easy to perform. However, we believe Fig. 7 serves us well for our purpose which is to examine the stability of the trap as a function of the power of the laser.

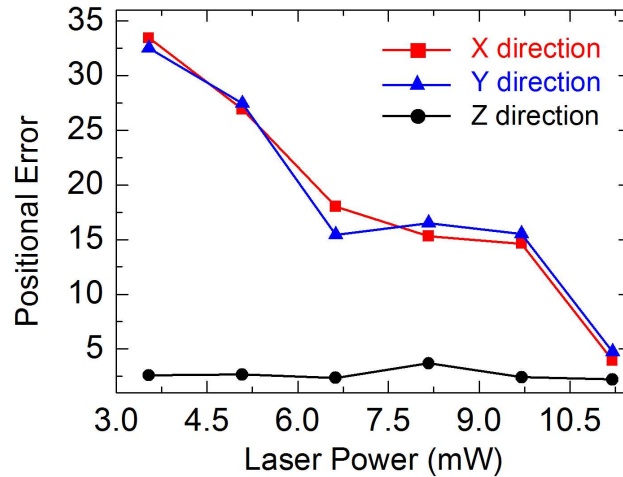


Fig. 7. Positional error of nanowires as function of the laser power. Vertical axis is in arbitrary unit.

It is evident that higher laser power results in less oscillation of the nanowire from the trap position. However, extremely high power can burn the conducting wires in the circuits when we approach them with trapped nanowires. We have found that 1mW was suitable to move and position nanowires to the assembly site using current levels of implementation. However, to fuse the nanowires to the gold conducting wires, we have to elevate the power to 3.5mW.

This developed and explained procedural method also demonstrates some inconsistencies. Specifically, the simultaneous fusion of both ends of the trapped nanowire to the conducting wires is not always easily achieved. Sometimes, one end would fuse first while the other end is left dangling. In these situations, it is occasionally possible to slightly rotate the nanowire so that the other end can further be fused. However, rotation is sometimes not possible as the fused end is quite rigidly grounded. We have also experienced a number of conducting wires which simply burned during the fusion process.

Nanowires can be trapped using two different modes depending on whether the angle formed between the nanowire and the laser beam axis is parallel or orthogonal. Parallel modes are addressed with stationary lasers, while orthogonal modes are addressed by scanning the

spot between the endpoints of a nanowire. We have conducted viscous drag force experiments to obtain the maximum trapping speed for each mode using $7\mu\text{m}$ nanowire under 1mW of laser power. Drag forces are produced by periodic movement of the microscope stage while holding the particle in a fixed trap. The scanning frequency is at 33Hz . For the first mode, maximum trapping speed is $61.5\mu\text{m}/\text{sec}$. For the second mode, these values are again dependent upon how the nanowire axis is oriented towards the medium flow direction. Two characteristic orientations are parallel and orthogonal. The obtained values are $27.9\mu\text{m}/\text{sec}$ and $25.4\mu\text{m}/\text{sec}$ for parallel and orthogonal, respectively. The obtained maximum trapping speeds for both directions are similar even though the hydrodynamic drag force for the orthogonal direction is much larger than the parallel direction due to the larger frontal area. But at the same time, the optical force for the orthogonal direction is also larger than the parallel direction. We think the optical force compensates for the hydrodynamic drag force, resulting in similar measurements.

4. Conclusion

Nanowires can be viewed as potential building blocks for various electronic devices with important applications and implications for the future. However, due to their small size, it is relatively difficult to manipulate them individually with high degrees of control and precision. In this study, we have shown a set of procedures by which we can manipulate a single In_2O_3 nanowire and then permanently fuse them on conducting gold wires. We have demonstrated two ways to trap nanowires. Firstly, nanowires are trapped and moved using single beams which are intensely focused on critical targets. We then use a line optical trap to place the nanowires where they are required. We have also demonstrated that nanowires can fuse to conducting wires by utilizing high-powered lasers. By demonstrating this, we are able to successfully surmise the I-V curves for the annealed and un-annealed nanowire samples. Optical manipulation and placement of nanowires in the construction of electric devices have been demonstrated by many authors. However, we want to emphasize the fact that there has been no effective demonstration of devices which focus on the flow of currents. We have bonded the indium-oxide nanowire using optical trapping onto pre-patterned electrodes that, for the first time, demonstrate diode-like, nonlinear characteristics of current-voltage. We believe our approach can have a significant impact on the usage of nanowires in the future.

Acknowledgments

This work has been supported by the Research Center for Biomolecular Nanotechnology and the institute of Medical System Engineering (iMSE) at GIST.